Proc. of JSCE,
No. 195, Nov. 1971

ANALYTICAL STUDY ON STRESS WAVE PROPAGATION IN VISCOELASTIC MATERIALS SUBJECTED TO SPIKE PULSE

By Koichi AKAI and Masayuki HORI***

1. INTRODUCTION

Comprehensive aseismatic design of structures should take behaviors of ground and the soil-structure interaction under seismic loading into account. This requirement has not been satisfied even partially because of the complexity in the mechanical properties of soil.

The authors have treated the propagation of stress wave in soil media as an approach to soil dynamics problems[1),2)]. In this study the authors have been so interested in the behavior of ground excited by the earthquake motion and wished to know what phenomena would occur at any point in the ground during the seismic disturbance, that the analytical method on the wave propagation theory has been used mainly in proceeding the study.

It is of great importance to investigate the damping characteristics of soil besides its strength behavior. For theoretical analysis of damping due to viscosity, it is usual to assume the viscoelastic damping mechanism[3),4)]. Assuming semi-infinite one-dimensional rods of some linear viscoelastic models, in the present paper, theoretical solutions are obtained for the stress propagation problems in the case of boundary stress forming a spike pulse with exponential decay.

2. PREVIOUS STUDIES

In general, during the propagation process of stress waves in soil, energy is absorpted by compaction (*i.e.*, intergranular friction) and viscosity of the soil. In explaining such an energy damping theoretically, various models are assumed. These models have been limited to simple ones, however, because of difficulty in solving the boundary value problems mathematically.

Seaman[5)] obtained the result from experimental data for one-dimensional stress wave in soil that the constant $\tan\delta$ model (purely viscoelastic dissipation) gave the best prediction of the wave for clay, and the viscoelastic compacting model for sand. The solution for the latter model was the first order approximation obtained from the elastic solution by using the correspondence principle. A comparison of wave propagation results and of theoretical prediction based on compression test properties showed that the arrival time of the stress wave could be predicted from the compression modulus of the soil, and that the stress attenuation could be predicted from the dissipative soil parameters found in the compression tests.

The stress and velocity distributions associated with the propagation of an impulsively applied velocity and stress along rods of viscoelastic materials were analysed by Morrison[6)] and by Lee and Morrison[7)]. Various viscoelastic materials were considered from the simple Voigt and Maxwell models up to a four-element model. The stress distribution for both cases of constant applied stress and constant applied velocity was represented graphically for the materials considered by using the Laplace transform technique.

Berry and Hunter[8)] solved the similar problem for the one-dimensional finite rod. In this study an account is given for the propagation of stress in thin viscoelastic rods when the ends of the rods satisfy a wide variety of boundary conditions. General solutions of the equations of motion are derived by use of the theory of Laplace transformations and their applicability demonstrated by the consideration of special problems.

The authors performed some theoretical studies on the one-dimensional stress propagation problems in cohesive soils[9)]. Theoretical models considered were Voigt model, Maxwell model and the standard linear viscoelastic model with three parameters. For these models there has not been any analytical solution except that for a step-pulse type boundary stress by Morrison *et al.* The authors obtained a solution for the latest model by using the principle

* Dr. Eng., Professor of Civil Engineering, Kyoto University
** M.S.C.E., Doctorial course student, Kyoto University

of superposition. In this method the surface stress forming a spike pulse of exponentially decaying type is uniformly divided into ten step-pulse type stresses, and the solution for each step is finally superposed with each other.

3. VOIGT MODEL AS A TWO-PARAMETER VISCOELASTIC MATERIAL

On beginning the discussion on the stress propagation in viscoelastic materials, we are concerned with a semi-infinite rod, $x\geq 0$, of Voigt-type material (Fig. 1) where the x-coordinate is measured along the length of the rod.

Introducing the dimensionless variables,

$$\xi=(\rho E)^{1/2}\mu x,\ \tau=E\mu t,\ \Sigma'=\sigma(x,t)/\sigma_0 \quad \cdots\cdots(1)$$

the fundamental equation for stress propagation is written as :

$$\Sigma_{\tau\tau}'=\Sigma_{\xi\xi}'+\Sigma_{\xi\xi\tau}' \quad \cdots\cdots(2)$$

where ρ denotes the density of the unstrained material, E the Young's modulus, μ the viscous constant, $\sigma(x,t)$ the nominal compressive stress, *i.e.*, the force per unit initial cross-sectional area transmitted across the section x of the rod, and the subscripts represent partial differentiation with respect to the corresponding variable.

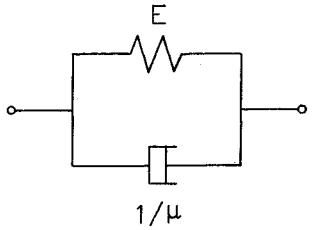

Fig. 1 Voigt model.

We take a spike pulse :

$$\Sigma'(\infty,\tau)=0,\ \Sigma'(0,\tau)=\exp(-\beta\tau) \quad \cdots\cdots(3)$$

as the boundary conditions, where $\beta=1/E\mu T_0$ (T_0: relaxation time). For $\beta=0$ the surface stress becomes to a step pulse, and $\beta=\infty$ corresponds to a single pulse.

Considering Laplace transformation :

$$L\{f(\xi,\tau)\}=\int_0^\infty e^{-s\tau}f(\xi,\tau)d\tau \quad \cdots\cdots(4)$$

then, Eq. (2) is reduced to the following ordinary differential equation.

$$s^2L\{\Sigma'\}=(1+s)L\{\Sigma'\}_{\xi\xi} \quad \cdots\cdots(5)$$

The transformations of the boundary conditions, Eq. (3), are

$$L\{\Sigma'(\infty,\tau)\}=0,\ L\{\Sigma'(0,\tau)\}=\frac{1}{s+\beta} \quad \cdots(6)$$

Solving Eq. (5) under the condition of Eqs. (6), we obtain

$$L\{\Sigma'(\xi,\tau)\}=\frac{1}{s+\beta}\exp\left\{\frac{-\xi s}{\sqrt{1+s}}\right\} \quad \cdots\cdots(7)$$

as the solution in the transformed field.

Using the integral formula, *i.e.*, if

$$\left.\begin{aligned}&\bar{x}(s)=L\{x(t)\}\ \text{and}\\&\phi(s)\exp\{-u\,\psi(s)\}=L\{K(t,u)\}\\&\text{then,}\\&\phi(s)\bar{x}\{\psi(s)\}=L\left\{\int_0^\infty K(t,u)x(u)du\right\}\end{aligned}\right\}\cdots(8)$$

we obtain the following final solution in the real field as the result of inversive transformation.

$$\Sigma'(\xi,\tau)=\frac{\xi}{2\sqrt{\pi}}\exp(-\beta\tau)\int_0^\tau\frac{g(\tau,\eta)}{\sqrt{\eta^3}}\cdot\exp\left\{(\beta+1)\eta-\frac{\xi^2}{4\eta}\right\}d\eta \quad \cdots\cdots(9)$$

where,

$$\left.\begin{aligned}&g(\tau,\eta)=\int_0^{\tau-\eta}\{\exp(\beta-1)t\}\cdot\left\{\delta(t)-\left(\frac{\eta}{t}\right)^{1/2}J_1(2\sqrt{\eta t})\right\}dt\\&J_1(2\sqrt{\eta t})=\sqrt{\eta t}\sum_{m=0}^{\infty}\frac{(-1)^m(\eta t)^m}{m!\Gamma(m+2)}\end{aligned}\right\}\cdots(9)'$$

In the special case for $\beta=0$ (step pulse) and $\beta=1$, one obtains the following solutions by using another type of transformation, respectively.

1) $\beta=0$:

$$\Sigma'(\xi,\tau)=\frac{e^{-\tau}}{\pi}\int_0^\tau\frac{\cos\{2\sqrt{\eta(\tau-\eta)}\}}{\sqrt{\eta(\tau-\eta)}}\cdot\exp\left(2\eta-\frac{\xi^2}{4\eta}\right)d\eta \quad \cdots\cdots(10)$$

2) $\beta=1$:

$$\Sigma'(\xi,\tau)=\frac{e^{-\tau}}{\pi}\int_0^\tau\left[\frac{\cos\{2\sqrt{\eta(\tau-\eta)}\}}{\sqrt{\eta(\tau-\eta)}}-\frac{\sin\{2\sqrt{\eta(\tau-\eta)}\}}{\eta}\right]\exp\left(2\eta-\frac{\xi^2}{4\eta}\right)d\eta \quad \cdots\cdots(11)$$

The solution (10) has been deduced by Morrison[6] for a step-pulse type boundary stress, and the difference from another solution (11) for a spike pulse with exponential decay is only the term of $\sin\{2\sqrt{\eta(\tau-\eta)}\}/\eta$ in parentheses. This means that the propagating stress attenuates more rapidly for a spike-pulse shock wave than for a step-pulse one.

Figs. 2 (a),(b) represent the stress solutions in Eqs. (10) and (11), respectively. The former was obtained by Morrison and the latter has been calculated by the authors, using Simpson's integrral formula with the integral intervals of 10^{-4}. For the numerical calculation FACOM 230-60 Digital Computer in Kyoto University was used. As is seen from the structural mechanism of Voigt model (Fig. 1), the instantaneous response to an impact results in a perfectly rigid behavior ; the wave front goes through the viscoelastic rod with infinite velocity. Besides, the attenuation time at every depth increases very rapidly with penetration of the

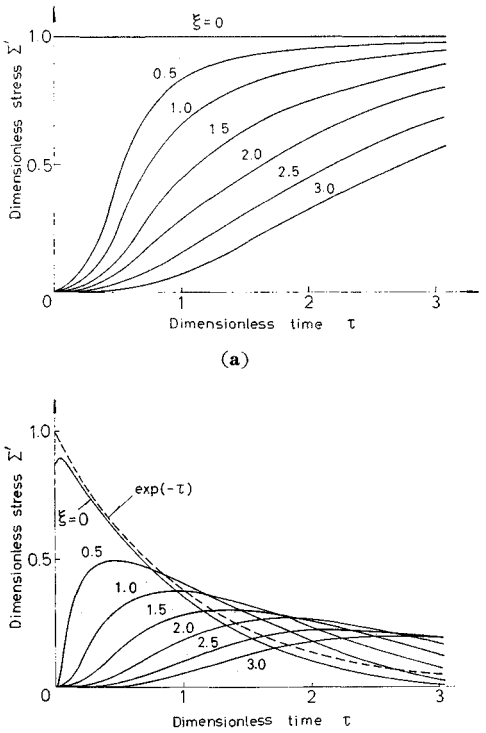

Fig. 2 Response of Voigt model to (a) step pulse and (b) spike pulse.

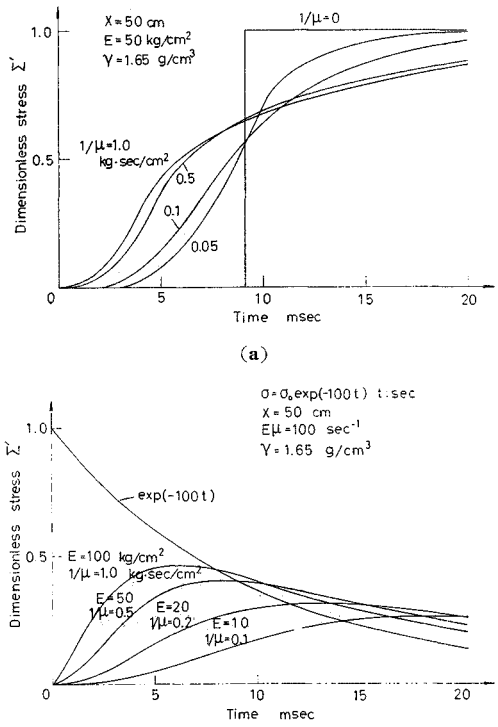

Fig. 3 Variation in wave form with viscoelastic constants in Voigt model under (a) step pulse and (b) spike pulse.

wave and there occurs very remarkable collapse of wave form. One can see a distinct difference on these characteristics between Voigt model and Maxwell model, both representing linear visco-elastic behaviors.

In these figures the effect of viscous damping on the wave propagation does not appear explicitly, because the abscissa and the parameter indicate the dimensionless time τ and dimensionless distance ξ, respectively, defined by Eq. (1). In order to examine the characteristics, we take the real time t as the abscissa and the coefficient of viscosity $1/\mu$ as the parameter.

Fig. 3 (a) indicates the pressure change at the position of $x=50$ cm when a step pulse is applied to the end of an infinite rod whose characteristics are explained by Voigt model with its Young's modulus $E=50$ kg/cm^2 and bulk density $\gamma=\rho g=1.65$ g/cm^3. The coefficient of viscosity is $1/\mu=0-1.0$ kg•sec/cm^2 : $1/\mu=0$ corresponds to a perfectly elastic material having no dash pot. In this case the wave front has a finite velocity and there exists no collapse of wave form, *viz.*, the step pulse transmits through the rod with its original shape. When existing a small amount of $1/\mu$, the theoretical wave velocity becomes infinite due to the mechanism of Voigt material. In actual, however, there appears finite velocity for small value of $1/\mu$. It takes much time, on the other hand, for the wave to reach peak stress when the value of $1/\mu$ increases.

Fig. 3 (b) is drawn for the spike-pulse type boundary stress similarly to Fig. 3 (a). In this figure we take the constant value of $E\mu=100$ sec^{-1}, and the stress form at $x=50$ cm is shown for the combination of E and $1/\mu$. From this figure it can be seen that the smaller the rheological constants $(E, 1/\mu)$ are, the flatter the stress wave becomes. The identical values of rheological constants in Figs. 3 (a) and (b) are $E=50$ kg/cm^2 and $1/\mu=0.5$ kg•sec/cm^2. As is known from comparison of curves in both figures, the stress wave propagating through material attenuates very rapidly in the case of boundary spike pulse which decays exponentially with time as already mentioned.

We turn our attention to the problem of response behavior of the dash pot in Voigt model. Investigating the coefficient of viscosity, $1/\mu$, the material can be considered as rigid body for $1/\mu\to\infty$, and the input energy propagates with finite velocity in the direction of rod length; there is no energy dissipation in the propagation process. If we take another extreme case of $1/\mu\to 0$, then the rate of strain ε_t becomes infinite so that the energy is

absorpted completely, thus there exists no energy propagation to the direction of rod length. In the latter case the absorpted energy propagates in the direction of time.

From the structural mechanism of Voigt meterial, it is recognized that for smaller value of $1/\mu$ the stresses are transmitted mainly by the spring E; the energy absorption is small and the collapse of wave is not remarkable. For large value of $1/\mu$, on the other hand, the stresses are transmitted mainly through the dash pot. In this case, however, the energy absorption is still small because of the large viscosity ; the stress propagation approaches the form of rigid meterial. Thus, the rate of propagating stress subjected to the spring and the dash pot varies due to the relative magnitude of them, and the value of $1/\mu$ at which the energy absorption becomes maximum is determined corresponding to a certain value of E.

4. SPRING-VOIGT MODEL AS A THREE-PARAMETER VISCOELASTIC MATERIAL

As described above it is impossible theoretically to explain the finite velocity in a medium and to express the acute rise of stress at the instance of arrival of the wave front, as long as we are concerned with Voigt model. Such a phenomenon can be explained generally by a rheological model in which a spring is put in series. Using the simplest Maxwell model (Fig. 4), however, the wave attenuation

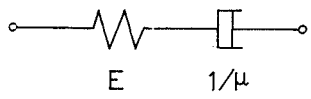

Fig. 4 Maxwell model.

is so rapid that the duration of wave motion cannot be expressed. Then, a three-parameter viscoelastic model is introduced to simulate characteristics that there occurs a discontinuous jump of stress in the neighbourhood of the surface of medium subjected to an impulsive loading and also to indicate the collapse of wave form behind the wave front.

We attempt to choose two kinds of true three-parameter linear viscoelastic model which express a finite wave velocity in general. One is the standard linear viscoelastic model shown in Fig. 5 (a) and the other is the spring-Voigt model in Fig. 5 (b). These models both consist of two springs and a dash pot, the constitutive equations being expressed as follows :

(a) Standard linear viscoelastic model

$$\frac{\sigma_t}{E'}+\mu\sigma=\varepsilon_t(1+k)+E\mu\varepsilon \quad \cdots\cdots(12)$$

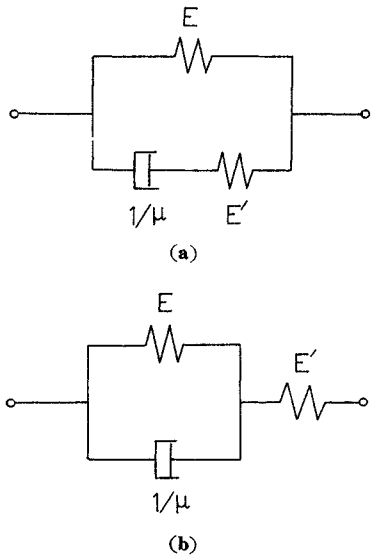

Fig. 5 Three-parameter viscoelastic models; (a) standard linear viscoelastic model and (b) spring-Voigt model.

(b) Spring-Voigt model

$$E\varepsilon+\frac{1}{\mu}\varepsilon_t=\sigma(1+k)+\frac{\sigma_t}{E'\mu} \quad \cdots\cdots(13)$$

where k is designated as

$$k=\frac{E}{E'} \quad \cdots\cdots(14)$$

Distinguishing both rheological constants by the subscripts a and b, above two models become identical by Morrison[6], provided the following correlation holds :

$$\frac{E_b}{E_a}=\frac{E_b'}{E_a'}=\sqrt{\frac{\mu_a}{\mu_b}}=1+\frac{E_a}{E_a'} \quad \cdots\cdots(15)$$

For the standard linear viscoelastic model defined by Eq. (12) Morrison[6] solved the wave propagation behavior under a step pulse, and the authors presented the response solution for a spike pulse ($\beta=1$) and $k=1$[9]. For the spring-Voigt model expressed by Eq. (13), on the other hand, the fundamental differential equation is written as follows, in terms of dimensionless parameter defined in Eq. (1).

$$\Sigma_{\xi\xi}'+\Sigma_{\xi\xi\tau}'=(1+k)\Sigma_{\tau\tau}'+k\Sigma_{\tau\tau\tau}' \quad \cdots\cdots(16)$$

Thus we obtain the following solution in the transformed field under the boundary condition Eq. (3) (Eq. (6) in transformed form).

$$L\{\Sigma'(\xi,\tau)\}=\frac{1}{s+\beta}\exp\left\{-\frac{s\sqrt{ks+k+1}}{\sqrt{s+1}}\xi\right\} \quad \cdots\cdots(17)$$

The solution in the real field by Laplace inversion theorem is :

$$\Sigma'(\xi,\tau)=\frac{1}{2\pi i}\int_{\gamma-i\infty}^{\gamma+i\infty}\frac{1}{s+\beta}e^{s\tau}\cdot\exp\left\{-\frac{s\sqrt{ks+k+1}}{\sqrt{s+1}}\xi\right\}ds \quad \cdots\cdots(18)$$

The integrand in Eq. (18) has a simple pole at $s=$

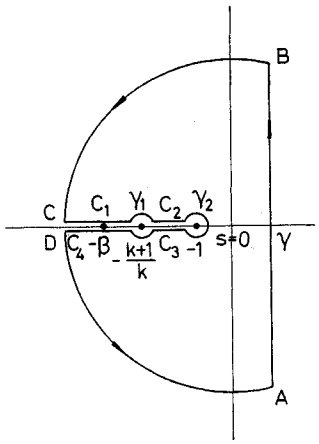

Fig. 6 Integral contour with the simple pole outside.

$-\beta$ and two branch points at $s=-1$ and $s=-(k+1)/k$. To evaluate this integral we complete the path of integration ABCDA as shown in Fig. 6, where ultimately the radii of two large circular quadrants tend to become infinite and the radii of the small circles tend to zero.

Following identical equation is defined :

$$I=\int\frac{1}{s+\beta}e^{s\tau}\exp\left\{-\frac{s\sqrt{ks+k+1}}{\sqrt{s+1}}\xi\right\}ds \cdots\cdots (19)$$

(1) In the case of $\beta>\frac{k+1}{k}$

Since the simple pole $s=-\beta$ is outside the contour, we have, by Cauchy's theorem,

$$\oint=I_{AB}+I_{BC}+I_{CD}+I_{DA}=0 \cdots\cdots (20)$$

so that,

$$I_{AB}=-I_{BC}-I_{CD}-I_{DA} \cdots\cdots (21)$$

Provided

$$\tau-\sqrt{k}\xi>0 \cdots\cdots (22)$$

then, by Jordan's lemma[10], the integrals around the two circular arcs tend to zero as the radii of the circles tend to infinity, *viz.*, $(I_{BC}+I_{DA})$ approaches zero. Thus, from Eq. (21), we are left with the equation

$$I_{AB}=-I_{CD} \cdots\cdots (23)$$

It is necessary to break up the integral from C to D into several parts, namely, the contours C_1 and C_4, C_2 and C_3, the circles γ_1 and γ_2.

1) Integral around the simple pole $s+\beta=0$:

For the integrals around the simple pole $s+\beta=0$ we write $s+\beta=\omega e^{i\theta}$, $|\theta|<\pi$, and substitute it into Eq. (19), which yields the result

$$I_\beta=-2\pi i e^{-\beta\tau}\exp\left\{\frac{\beta\sqrt{k\beta-k-1}}{\sqrt{\beta-1}}\xi\right\} \cdots\cdots (24)$$

2) Integral along C_1 and C_4 :

We write

$$\{g(s)\}^2=\frac{s^2(ks+k+1)}{s+1} \cdots\cdots (25)$$

which is schematically illustrated in Fig. 7. From

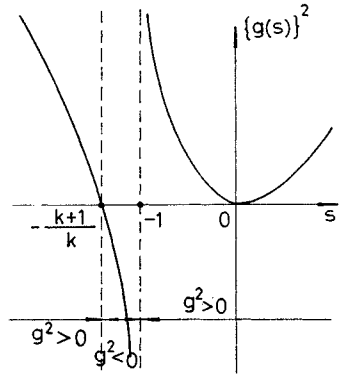

Fig. 7 Functional form of $g(s)$.

this figure, since $g(s)$ is a single-valued function along C_1 and C_4, the sum contribution from these two paths is zero. That is,

$$I_{C_1}+I_{C_4}=0 \cdots\cdots (26)$$

3) Integral around the circle γ_1 :

For the integral around the circle γ_1 enclosing the branch point $s+\frac{k+1}{k}=0$, we write $s+\frac{k+1}{k}=\omega e^{i\theta}$, and substitute it into Eq.(19), then it can be shown that

$$I_{\gamma_1}=\lim_{\omega\to 0}\int_{-\pi}^{\pi}\exp\left\{-\frac{k+1}{k}\tau\right\}\cdot\exp\left\{\frac{k+1}{k}\frac{\sqrt{k\omega e^{i\theta}}}{\sqrt{1-\frac{k+1}{k}}}\xi\right\}\frac{\omega ie^{i\theta}}{\beta-\frac{k+1}{k}}d\theta=0 \cdots\cdots (27)$$

4) Integral around the circle γ_2 :

For the integral around the circle γ_2 enclosing the branch point $s+1=0$, we write $s+1=\omega e^{i\theta}$, and substitute it into Eq. (19), then it becomes

$$I_{\gamma_2}=\lim_{\omega\to 0}[1+0(\omega)]\int_{-\pi}^{\pi}e^{-\tau}\exp\left\{\frac{1}{\sqrt{\omega}e^{1/2\cdot i\theta}}\right\}\frac{\omega ie^{i\theta}}{\beta-1}d\theta$$
$$=\frac{2\pi i}{\beta-1}\xi^2e^{-\tau} \cdots\cdots (28)$$

5) Integral along C_2 and C_3 :

Finally along C_2 and C_3 we put $s+1=qe^{i\pi}$ and $s+1=qe^{-i\pi}$, respectively, to obtain the contribution,

$$I_{C_2}+I_{C_3}=2\int_0^{1/k}\frac{1}{q+1-\beta}e^{-(q+1)\tau}\cdot\sin\left\{\frac{(q+1)\sqrt{1-kq}}{\sqrt{q}}\xi\right\}dq \cdots\cdots (29)$$

From Eqs. (18), (23), (24), (26), (27), (28) and (29) we obtain the final solution as follows :

$$\Sigma'(\xi,\tau)=e^{-\beta\tau}\exp\left\{\frac{\beta\sqrt{k\beta-k-1}}{\sqrt{\beta-1}}\xi\right\}-\frac{1}{\beta-1}\xi^2e^{-\tau}-\frac{1}{\pi}\int_0^{1/k}\frac{1}{q+1-\beta}e^{-(q+1)\tau}\cdot\sin\left\{\frac{(q+1)\sqrt{1-kq}}{\sqrt{q}}\xi\right\}dq \cdots\cdots (30)$$

(2) In the case of $\frac{k+1}{k}\geq\beta>1$

Instead of Eq. (24), having the following contri-

bution,

$$I_\beta=-2\pi i e^{-\beta\tau}\cos\left\{\frac{\beta\sqrt{k+1-k\beta}}{\sqrt{\beta-1}}\xi\right\} \quad \cdots\cdots(31)$$

we obtain the solution

$$\Sigma'(\xi,\tau)=e^{-\beta\tau}\cos\left\{\frac{\beta\sqrt{k+1-k\beta}}{\sqrt{\beta-1}}\xi\right\}-\frac{1}{\beta-1}\xi^2e^{-\tau}-\frac{1}{\pi}\int_0^{1/k}\frac{1}{q+1-\beta}e^{-(q+1)\tau}\cdot\sin\left\{\frac{(q+1)\sqrt{1-kq}}{\sqrt{q}}\xi\right\}dq \quad \cdots\cdots(32)$$

(3) In the case of $\beta=1$

Substituting $\beta=1$ into Eq. (19), it reduces to

$$I=\int\frac{1}{s+1}e^{s\tau}\exp\left\{-\frac{s\sqrt{ks+k+1}}{\sqrt{s+1}}\xi\right\}ds \quad \cdots(33)$$

In this case the simple pole lies on the branch point $s+1=0$. It is necessary to determine the residue of the integrand in Eq. (33) at $s=-1$ in order to know the contribution around the simple pole. It is self-evident, however, that the residue equals unity. The contributions on the remaining contour are obtained by the same way as that in the case (1) or (2). Therefore we obtain the solution

$$\Sigma'(\xi,\tau)=1-\frac{1}{\pi}\int_0^{1/k}\frac{1}{q}e^{-(q+1)\tau}\cdot\sin\left\{\frac{(q+1)\sqrt{1-kq}}{\sqrt{q}}\xi\right\}dq \quad \cdots(34)$$

(4) In the case of $0\leq\beta<1$

Since the simple pole $s=-\beta$ is inside the contour ABCDA as shown in Fig. 8, we have by Cauchy's theorem,

$$\oint=I_{AB}+I_{BC}+I_{CD}+I_{CD}=2\pi i \quad \cdots\cdots(35)$$

so that,

$$I_{AB}=2\pi i-I_{BC}-I_{CD}-I_{DA} \quad \cdots\cdots(36)$$

By Jordan's lemma we have

$$I_{BC}+I_{DA}=0 \quad \cdots\cdots(37)$$

Substituting Eq. (37) into Eq. (36), it reduces to

$$I_{AB}=2\pi i-I_{CD} \quad \cdots\cdots(38)$$

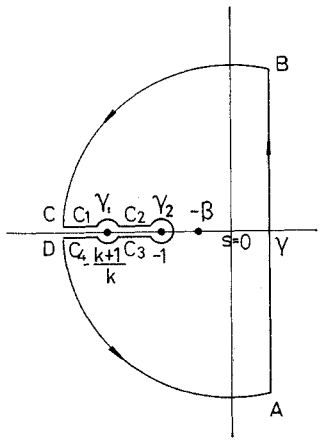

Fig. 8 Integral contour with the simple pole inside.

By the same way as the case (1) or (2), we have

$$I_{CD}=\frac{2\pi i}{\beta-1}\xi^2e^{-\tau}+2i\int_0^{1/k}\frac{1}{q+1-\beta}e^{-(q+1)\tau}\cdot\sin\left\{\frac{(q+1)\sqrt{1-kq}}{\sqrt{q}}\xi\right\}dq \quad \cdots\cdots(39)$$

and the solution

$$\Sigma'(\xi,\tau)=1-\frac{1}{\beta-1}\xi^2e^{-\tau}-\frac{1}{\pi}\int_0^{1/k}\frac{1}{q+1-\beta}e^{-(q+1)\tau}\cdot\sin\left\{\frac{(q+1)\sqrt{1-kq}}{\sqrt{q}}\xi\right\}dq \quad \cdots(40)$$

The condition Eq. (22) to satisfy Jordan's lemma is one in the range $\mathrm{Re}(s)<0$. If we consider a contour in the range $\mathrm{Re}(s)>0$, however, the condition to satisfy Jordan's lemma is

$$\tau-\sqrt{k}\xi<0 \quad \cdots\cdots(41)$$

Since we have no singular point in the range $\mathrm{Re}(s)>0$, the integral I along the contour is always zero. That is, the range repsesented by Eq. (41) is a part in which the wave does not arrive. Also, the boundary between two ranges, *i.e.*, $\tau-\sqrt{k}\xi>0$ and $\tau-\sqrt{k}\xi<0$, represents the wave front.

We have the reduction, by using the original constants, E, E' and μ, and variables, t and x, standing for the dimensionless variables τ and ξ,

$$\tau=\sqrt{k}\xi$$

$$i.e.,\ E\mu t=\sqrt{\frac{E}{E'}}(\rho E)^{1/2}\mu x$$

$$\therefore\ \frac{x}{t}=\sqrt{\frac{E'}{\rho}} \quad \cdots\cdots(42)$$

This indicates nothing but the velocity of wave front.

5. CONSIDERATION AND DISCUSSION ON CALCULATED RESULTS

The numerical calculations are performed with an aim to determine the collapse of the wave form in the spring-Voigt model, *i.e.*, attenuation of peak stress and increase in rise time, and to compare them with the experimental results in this study.

First we take the simple Voigt model (Fig. 1)

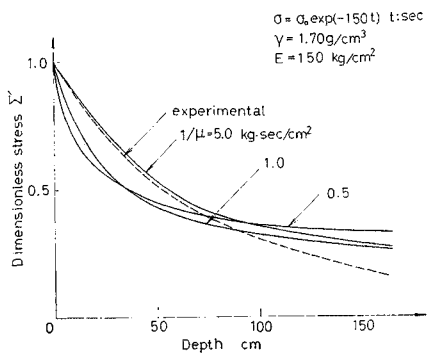

Fig. 9 Comparison of experimental with theoretical results (Voigt model).

described in **3.** for which the solution of propagating stress wave is given by Eqs. (9) and (9)′. Calculated results for some variation in the coefficient of viscosity $1/\mu$ are shown in Fig. 9, which is computed under the following conditions : the surface load $\sigma=\sigma_0 \exp(-150\,t)$ (t : sec), the bulk density $\gamma=\rho g=1.70\,\mathrm{g/cm^3}$, Young's modulus $E=150\,\mathrm{kg/cm^2}$. Experimental results for sandy loam by the shock tube test described elsewhere[11] are plotted in this figure. According to this results, the fitting of the rheological constants, $E=150\,\mathrm{kg/cm^2}$ and $1/\mu=5.0\,\mathrm{kg\cdot sec/cm^2}$ satisfactorily explains the stress attenuation behavior until the distance $x\fallingdotseq 60$ cm. For larger distance the attenuation obtained in experiment is rather larger than that expected by theoretical calculation.

As an example of numerical calculations for the spring-Voigt model (Fig. 5(b)), we choose here the decaying parameter $\beta=5$. The calculations are carried out with the Young's modulus ratio k in the range of 0.5 to 3.5. Such values of parameters β and k are roughly predicted from the experimental results on the stress propagation in soil using the shock tube technique. The calculated results using FACOM 230-60 Digital Computer are given in Fig. 10, showing the attenuation of peak stress. There seems no variation in rise time, *viz.*, there is a

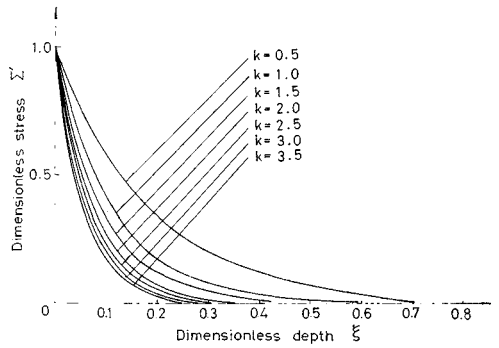

Fig. 10 Calculated results for attenuation of peak stress in spring-Voigt model ($\beta=5.0$).

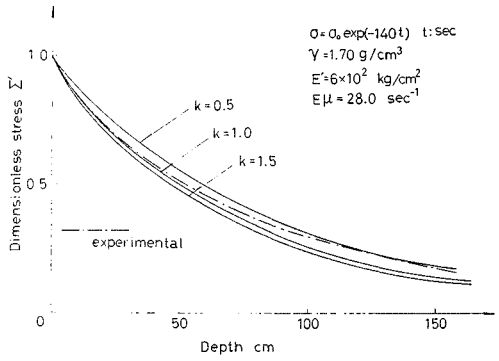

Fig. 11 Comparison of experimental with theoretical results (spring-Voigt model).

shock front even when the wave proceeds into greater depth and the peak stress occurs at the wave front. Furthermore, the wave form at the boundary surface almost does not collapse as the wave goes down. From this figure one can see that the attenuation along the dimensionless depth ξ increases with increase in the parameter k. The increase in k implies the decrease in Young's modulus E' of the free spring with respect to another spring E in the spring-Voigt model. The above phenomenon can be understood by taking the fact into account, therefore, that Voigt behavior mainly appears with increase in the parameter k.

Now we compare our results of analysis with the experimental attenuation of stress. Since the velocity of stress wave in the spring-Voigt model is given by $\sqrt{E'/\rho}$, we regard E' as the confined modulus computed by ρc^2 (ρ : density, c : celerity) in order to fit the theoretical result to the experimental velocity. We choose $E'=6\times10^2\,\mathrm{kg/cm^2}$ for the bulk density $\gamma=1.70\,\mathrm{g/cm^3}$. Furthermore, we use a typical value of the decaying parameter $\alpha=140\,\mathrm{sec^{-1}}$ taking the fact into consideration that the attenuation does not depend on the applied pressure level. The calculated results for $\beta=5.0$ are indicated in Fig. 11, in which the corresponding attenuation in experiments is also represented. From this figure one can see that the theoretical results for a given Young's modulus and bulk density do not vary regardless of E and μ, and that the theoretical solutions for $k=0.5-1.0$ very well express the experimental results.

From this consideration we reach some important conclusion. That is, the use of the spring-Voigt model to soil subjected to an impulsive disturbance gives us better prediction of one-dimensional stress propagation. It comes from two viewpoints ; one is that there exists little variation in rise time in both experimental and theoretical results, namely, the wave form at the boundary surface does not collapse as the wave goes down, and the other is that the stress attenuation predicted by the theory well coincides with the experimental one. It is also noted that the attenuation in the spring-Voigt model depends on the product of E and μ as well as E', but not E and μ, individually.

6. CONCLUSION

In the present study, in order to obtain the analytical solution to stress propagation problems in the ground in which the damping effect of soil is considered, the one-dimensional response of cohesive soil subjected to an impulsive stress of spike pulse with exponential decay is calculated, and the adapta-

bility of the theory is investigated through the experimental data. The main conclusions obtained are summarized as follows：

(1) The stress propagation in Voigt material subjected to an impulse of step pulse or spike pulse at its end can be calculated analytically by using the Laplace transform technique. Comparing the attenuation behaviors with respect to the type of impulse, the stress wave propagating through material attenuates very rapidly in the case of boundary spike pulse which decays exponentially with time.

(2) In Voigt material the instantaneous response to an impact results in a perfectly rigid behavior. The duration time at every depth increases very rapidly with penetration of the wave, on the other hand, and there occurs very remarkable collapse of wave form. The rate of propagating stress subjected to the spring E and the dash pot $1/\mu$ varies due to the relative magnitude of them, and the value of $1/\mu$ at which the energy absorption is maximum is determined corresponding to a certain value of E.

(3) Three-parameter viscoelastic models are introduced to simulate characteristics that there occurs a discontinuous jump of stress in the neighbourhood of the surface of medium subjected to an impulsive loading and also indicates the collapse of wave form behind the wave front. These are the standard linear viscoelastic model and the spring-Voigt model, and for the latter, the analytical solutions are presented using the inversive Laplace transformation with the mean of contour integral. These results are compared with experimental data, and the discussion indicates that the analytical solution satisfactorily explains the attenuation behavior of confined soils.

The authors are greatly indebted to Mr. T. Shimogami, graduate student in Kyoto University, in performing numerical calculations for Voigt-type material.

REFERENCES

1) Akai, K., Tokuda, M. and T. Kiuchi：Experimental Study on the Propagation of Stress Wave in Cohesive Soils, Proc. JSCE, No. 161, 1969, pp. 59-67.
2) Akai, K. and M. Hori：Basic Study on the Dynamic Soil-Structure Interaction, Proc. JSCE, No. 173, 1970, pp. 61-78.
3) Krizek, R.J. and A.G. Franklin：Energy Dissipation in a Soft Clay, Proc. Intern. Symp. Wave Propagation and Dynamic Properties of Earth Materials, 1967, pp. 797-807.
4) Akai, K.：Damping Characteristics of Saturated Clay Subjected to Impact or Vibration, Proc. 14th Japan Congr. Materials Research, 1971, pp. 174-176.
5) Seaman, L.：One-Dimensional Stress Wave Propagation in Soils, Stanford Research Inst., AD-632106, DASA 1757, 1966, pp. 1-163.
6) Morrison, J.A.：Wave Propagation in Rods of Voigt Material and Visco-Elastic Materials with Three-Parameter Models, Q. Appl. Math., Vol. 14, 1956, pp. 153-169.
7) Lee, E.H. and J.A. Morrison：A Comparison of the Propagation of Longitudinal Waves in Rods of Viscoelastic Materials, J. Polymer Sci., Vol. 14, 1956, pp. 93-110.
8) Berry, D.S. and S.C. Hunter：The Propagation of Dynamic Stresses in Visco-Elastic Rods, J. Mech. and Phys. of Solids, Vol. 4, 1956, pp. 72-95.
9) Akai, K. and M. Hori：A Viscoelastic Approach to the Problem of Stress Wave Propagation in Cohesive Soils, Proc. JSCE, No. 185, 1971, pp. 95-103.
10) Thomson, W.T.：Laplace Transformation, Maruzen, 1960, pp. 232-234.
11) Akai, K. and M. Hori：Considerations on Stress Propagation Characteristics through Soil by Means of Shock Tube Test, Preprint of 6th Japan Conf. SMFE, 1971 (in Japanese).

(*Received May 6, 1971*)